Front. Earth Sci. 2024, 18(3): 611−622
https://doi.org/10.1007/s11707-024-1098-x

RESEARCH ARTICLE

# Sequence stratigraphic analysis of superimposed coal measure gas-bearing system in Daning-Jixian block, eastern margin of Ordos Basin, China

**Shizhuang YANG[1,2], Song LI (✉)[1,2], Wenguang TIAN[3], Guanghao ZHONG[1,2], Junjian WANG[4]**

1 School of Energy Resources, China University of Geosciences (Beijing), Beijing 100083, China
2 Coal Reservoir Laboratory of National Engineering Research Center of CBM Development & Utilization, Beijing 100083, China
3 PetroChina Research Institute of Petroleum Exploration & Development, Beijing 100083, China
4 Klohn Crippen Berger Ltd., Brisbane, Queensland 4101, Australia



**Abstract** The identification of superimposed gas-bearing systems in coal measures is the basis for expediting the optimization of coal measure gas co-production. Through the analysis of drill cores and log data of Upper Carboniferous Benxi Formation to the member 8 of Middle Permian Lower Shihezi Formation in Daning-Jixian block, eastern margin of Ordos Basin, four distinct superimposed coal measure gas-bearing systems were identified, and their formation mechanism was discussed from the sequence stratigraphic perspective. Type I system mainly contains multiple coal seams, shales and sandstone layers. Type II system is dominated by multiple coal seams and shales. Type III is characterized by multiple sandstone layers, and type IV system is dominated by limestones and mudstones. In general, the gas-bearing systems deposited in barrier-lagoon are type II, those deposited in carbonate tidal flats are type IV, and those deposited in the delta front are types I and III. The marine mudstone, acting as a key layer near the maximum flooding surface, exhibits very low permeability, which is the main factor contributing to the formation of superimposed gas-bearing systems. The sedimentary environment plays a significant role in controlling the distribution of gas-bearing systems. Notably, the vertical gas-bearing systems in the south-western region, where delta front and lagoon facies overlap, are more complex than those in the north-eastern delta front facies.

**Keywords** coal measure gas, superimposed gas-bearing system, sequence stratigraphic, key layer

Received March 26, 2023; accepted July 21, 2023

E-mail: lisong@cugb.edu.cn

## 1 Introduction

In recent years, China's energy sector has paid extensive attention to the commercial potential of coal measure gas resource (Zou et al., 2019; Su et al., 2020). However, in coal measures, the reservoirs and cap layers are frequently superimposed, resulting in the coexistence of multiple pressure systems and the compatibility issues for co-production, limiting gas production from individual wells (Li et al., 2023a). Therefore, identifying gas-bearing systems is crucial for efficient development of coal measure gas.

Previous studies on the superpositionality of gas-bearing systems has been carried out from various perspectives, including reservoir pressure (Powley, 1990; Chen et al., 2018a), gas content vertical fluctuations (Lei et al., 2012; Wang et al., 2015), hydrogeological conditions (Su et al., 2005; Yang et al., 2015), production dynamics (Tang et al., 2017; Jia et al., 2021), and sedimentary stratigraphy (Martin et al., 1997; Allen and Fielding, 2007; Wang et al., 2020). The study of sequence stratigraphy under epicontinental-sea environments further reveals the formation mechanism of superimposed gas-bearing systems in coal measures. Depositional systems in such environments differ from river-dominated systems due to frequent influences from waves and tides (Cooper et al., 2018; Nowacki and Ganju, 2018; Raff et al., 2018), resulting in the formation of sequence stratigraphy with certain rhythms in the coal-bearing basins at different evolutionary stages. Differences in the systems tracts affect the environment, characteristics, and intensity of coal accumulation and also make the lithology of associated rocks significantly different (Flores and Sykes, 1996; Diessel et al., 2000; Holz et al., 2002; Wang et al.,

2019). These variations affect the gas content and seepage capacity of coal reservoirs (Shen et al., 2016), and the development of water-barrier and gas-barrier layers separates gas-bearing units in coal measures, forming distinct gas-bearing systems (Shen et al., 2017). Due to the complexity of geological conditions, there are significant differences in distribution, overlap frequency, and controlling factors of coal measures gas-bearing systems in different regions. However, there is still a need for systematic and in-depth discussions on superimposed gas-bearing systems of coal measures gas from a sedimentary perspective.

In this study, the vertical distribution characteristics of geological conditions are analyzed in details to identify the superimposed gas-bearing systems in Daing-Jixian block of the Ordos Basin. Combined with sequence stratigraphic framework division and sedimentary facies analysis, the formation mechanism of superimposed gas-bearing systems in coal measures is clarified. The outcome of this study is important for optimization of coal measure gas co-production.

## 2 Geological setting

The Daning-Jixian block is located in the southeast of Ordos Basin, specifically in the southern part of Jinxi flexure fold belt on the eastern margin of the basin (Zhong et al., 2022; Li et al., 2023b; Fig. 1(a)). The strata in Daning-Jixian block are predominantly horizontal orientation, with localized faults development. The study area is about 25 km long from north to south, 22 km wide from east to west, with a total area of about 5.5 × $10^2$ $km^2$ (Fig. 1(b)).

The coal measures of the Daning-Jixian block consist of the Upper Carboniferous Benxi ($C_2b$), Taiyuan ($C_2t$), the Permian Shanxi ($P_1s$), and the member 8 of Lower Shihezi ($P_2x_8$) Formations. $C_2b$ was deposited in the early Late Paleozoic, and $C_2t$ is in direct contact with the underlying $C_2b$. The limestone at the bottom of $C_2t$ is Maoergou limestone, and the limestone at the top is known as Dongdayao limestone (Wang et al., 2022). Peitsakou sandstone is a marker layer at the bottom of $P_1s$, with gray pebbled sandstone and quartz sandstone. Lotopo sandstone is a marker layer at the base of $P_2x_8$. A total of 10 coal seams are developed in the area, among which No. 5 coal seam of $P_1s$ and No. 8 coal seam of $C_2t$ are stably distributed, which are the main coal seams in the area. In contrast, the other coal seams have significant structural changes and are varying in thicknesses. The thickness of No. 5 coal seam in $P_1s$ is 1.5−7.2 m, with an average thickness of 3.18 m. The thickness of No. 8 coal

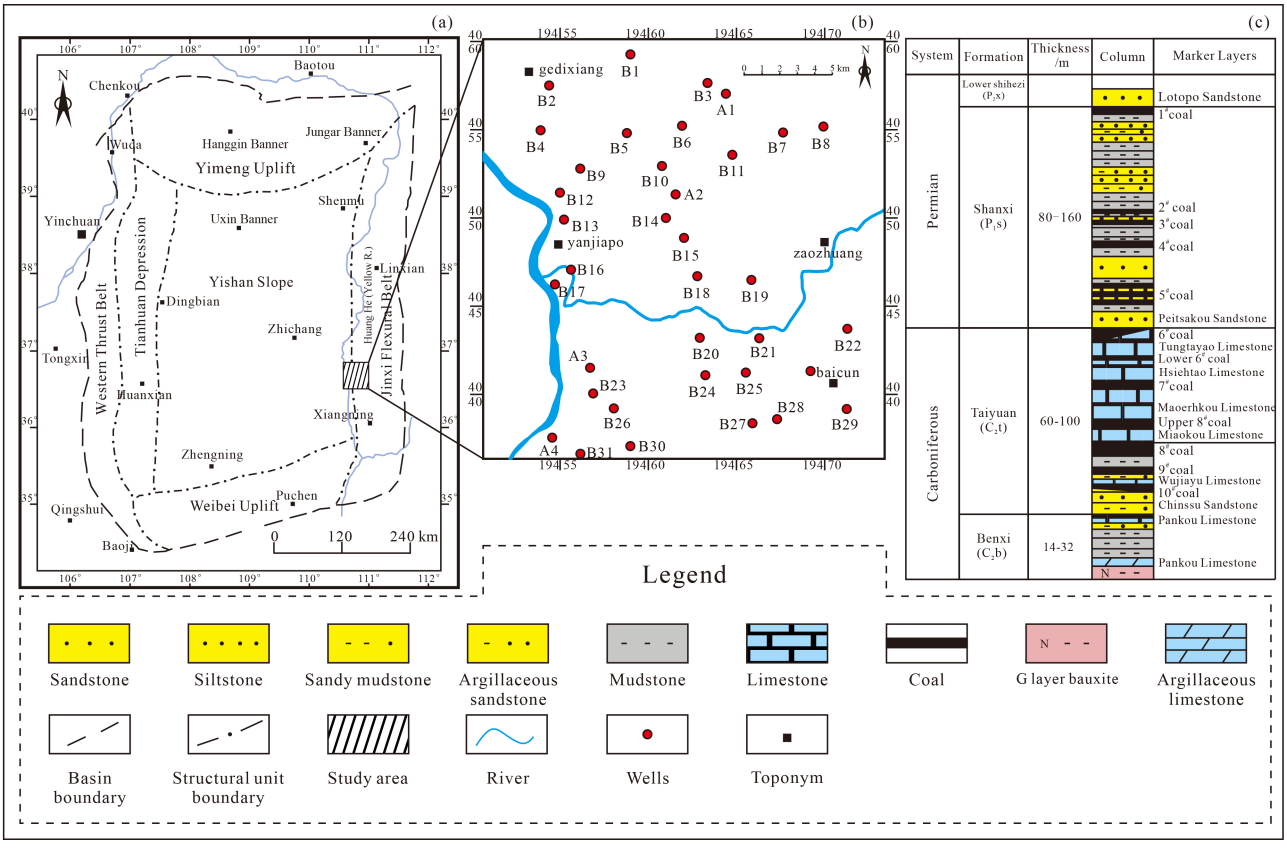


**Fig. 1** Location of the Daning-Jixian block. (a) Location of the Daning-Jixian block in the Ordos Basin; (b) Locations of the well sites studied in Daning-Jixian block; (c) Composite stratigraphic column showing coal-bearing formations in Daning-Jixian block.

seam in $C_2t$ is 2.0–9.8 m, with an average thickness of 4.5 m (Fig. 1(c)).

## 3 Identification of superimposed gas-bearing systems

### 3.1 Reservoir pressure coefficient

The main characteristic of an independent gas-bearing system is its well-integrated fluid pressure system (Li et al., 2023a). The Eaton method is an empirical method for predicting formation pressure coefficient by using the actual measured formation pressure as the constraint (Eaton,1972). By establishing the normal compaction trend line, the magnitude of formation pore pressure is calculated for mudstone and sandstone formations when the actual logging data deviate from the normal compaction trend line. The formulas are as follows:

$$P_f = OBG - ((OBG - P_n) \times (\mathrm{d}T_n/\mathrm{d}T_o)^c), \quad (1)$$

$$c = \frac{\ln(p_0 - p_\mathrm{p})/(p_0 - p_\mathrm{a})}{\ln(\mathrm{d}T_\mathrm{n}/\mathrm{d}T_\mathrm{o})}, \quad (2)$$

where $\rho_\mathrm{p}$ is the strata pressure equivalent density, g/cm$^3$; $\rho_0$ is the overlying strata pressure equivalent density, g/cm$^3$; $\rho_\mathrm{w}$ is the density of stratified water, g/cm$^3$; $\mathrm{d}T_\mathrm{n}$ is the normal compaction acoustic time difference, μs/m; $\mathrm{d}T_\mathrm{o}$ is the measured acoustic time difference, μs/m; $c$ is the Eaton coefficient, $P_0$ is the overburden pressure, MPa; $P_\mathrm{P}$ is the measured pressure, MPa; and $P_\mathrm{a}$ is the hydrostatic pressure, MPa.

The comparison of the calculations with the measured pressure coefficients shows that the error is less than 10% (Fig. 2).

In this study, the upper Paleozoic pressure in the basin was classified into four types: abnormally low pressure (pressure coefficient < 0.9), low pressure (pressure coefficient between 0.9 and 0.96), normal pressure (pressure coefficient between 0.96 and 1.06), and high pressure (pressure coefficient between 1.06 and 1.2). Calculations show that the pressure coefficient of $C_2b$ to $P_2x_8$ in the study area ranges from 0.36 to 1.10, with a concentration of between 0.75 and 0.98, and with low pressure and normal pressure predominant. Pressure coefficients stays constant from the top of $C_2b$ to the top of the member $2^2$ of Shanxi Formation ($P_1s_{2\text{-}2}$) and sharply decrease to a low value from the top of $P_1s_{2\text{-}2}$ to the bottom of the member $2^1$ of Shanxi Formation ($P_1s_{2\text{-}1}$). Pressure coefficients stays constant from the bottom of $P_1s_{2\text{-}1}$ to the top of the member 1 of Shanxi Formation ($P_1s_1$) and sharply decline from the top of $P_1s_1$ to the bottom of $P_2x_8$ (Fig. 3). Therefore, the pressure system from $C_2b$ to $P_2x_8$ in the study area can be divided into three separate gas-bearing systems: 1) from the top of $C_2b$ to the top of $P_1s_{2\text{-}2}$, 2) from the bottom of $P_1s_{2\text{-}1}$ to the top of $P_1s_1$, and 3) from the bottom of $P_2x_8$ to the top of $P_2x_8$.

### 3.2 Gas content

The vertical variation of gas content serves as a crucial indicator to classify the vertical gas system (Zhang et al., 2015; Chen et al., 2018b). Based on the statistics of gas measurement data, the distribution of total hydrocarbon is depicted to characterize the vertical variation of gas-bearing property. According to the relationship between total hydrocarbon value and burial depth in A4 wells, it can be seen that the total hydrocarbon value can be divided into four stages: 1) from the top of $C_2b$ to the top of the member 2 of Taiyuan Formation ($C_2t_2$), 2) from the bottom of the member 1 of Taiyuan Formation ($C_2t_1$) to the top of $P_1s_{2\text{-}2}$, 3) from $P_1s_{2\text{-}1}$ to the top of $P_1s_1$, and 4) from the bottom of $P_2x_8$ to the middle of $P_2x_8$. The total hydrocarbon values increase and then decrease with increasing burial depth, with noticeable drop-off sections between each section. Moreover, the magnitude of vertical fluctuation of gas content varies, indicating that the independent gas-bearing systems are developed in different layers (Fig. 4).

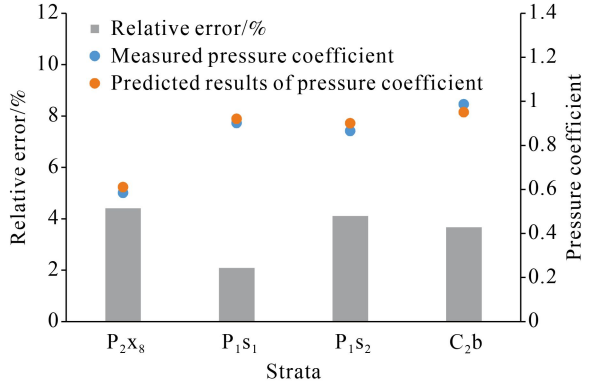


**Fig. 2** Comparison of calculated and measured pressure coefficients.

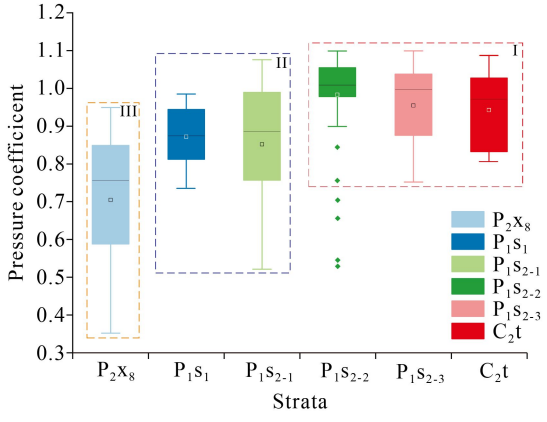


**Fig. 3** Box plot of pressure coefficient in well B22.

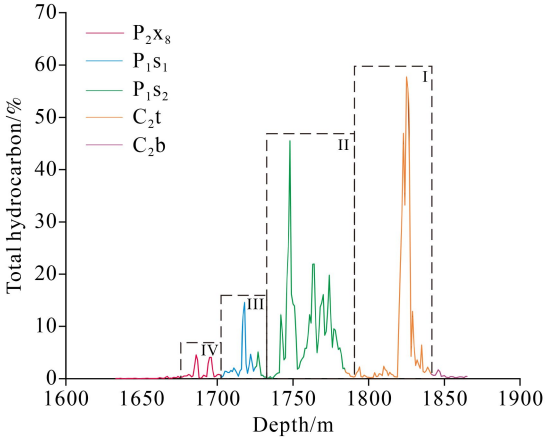


**Fig. 4** Variation curve of total hydrocarbon values with depth in well A4.

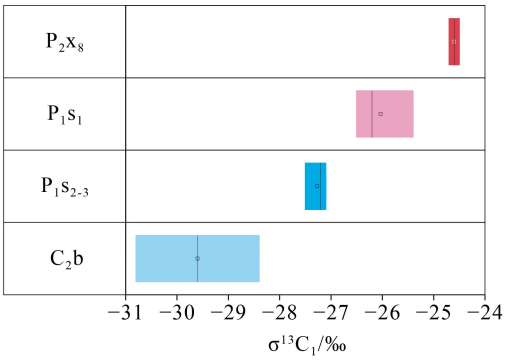


**Fig. 5** Carbon isotope distribution characteristics of natural gas in Daning-Jixian block.

### 3.3 Fluid geochemical characteristics

The fluid geochemical characteristics could be used to distinguish gas-bearing systems (Guo et al., 2020; Zhang et al., 2022). A comparison of natural gas carbon isotope test results from 10 wells in the study area shows that the average $\delta^{13}C_1$ value of $C_2b$ in Daning-Jixian block is −31.7‰. The average $\delta^{13}C_1$ value of $P_1s_{2-3}$ is −27.27‰. The average $\delta^{13}C_1$ value of $P_1s_1$ is −26.03 ‰ and the average $\delta^{13}C_1$ value of $P_2x_8$ is −24.6‰ (Table 1).

The carbon isotopes of methane in the study area progressive increase in weight from $C_2b$ to $P_2x_8$ (Fig. 5). It is evident from the figure that there is a pronounced differentiation in carbon isotope composition among the natural gas samples in the Daning-Jixian block. The carbon isotopes of natural gas are significantly heavier in $P_1s_{2-3}$ than in $C_2b$, suggesting that the fluid in $P_1s_{2-3}$ may not have communicated with the fluid in $C_2b$. The carbon isotopes of natural gas are significantly heavier in $P_1s_1$ than in $P_1s_{2-3}$, and they are heavier in $P_2x_8$ than in $P_1s_1$. As a result, between $P_1s_1$ and $P_1s_{2-3}$, and between $P_2x_8$ and $P_1s_1$, low permeable layers could hinder the fluid communication between the overlying and underlying strata.

**Table 1** Natural gas carbon isotope statistics

| Well | Strata | Sample type | $\delta^{13}C_1$/‰ |
|---|---|---|---|
| B21 | $P_2x_8$ | Saline bottle gas sample | −24.5 |
| B17 | $P_2x_8$ | Saline bottle gas sample | −24.7 |
| B3 | $P_1s_1$ | Saline bottle gas sample | −26.2 |
| B18 | $P_1s_1$ | Saline bottle gas sample | −26.5 |
| B23 | $P_1s_1$ | Saline bottle gas sample | −25.4 |
| B30 | $P_1s_{2-3}$ | Saline bottle gas sample | −27.1 |
| B27 | $P_1s_{2-3}$ | Saline bottle gas sample | −27.5 |
| B21 | $P_1s_{2-3}$ | Saline bottle gas sample | −27.2 |
| B31 | $C_2b$ | Saline bottle gas sample | −30.8 |
| B14 | $C_2b$ | Saline bottle gas sample | −32.6 |

### 3.4 Gas-bearing system identification

Ensuring the accuracy of gas-bearing system classification in the study area requires a comprehensive assessment of multiple factors, including the consistency of reservoir pressure coefficients and natural gas geochemical characteristics. Although this consistency is necessary, it is not sufficient on its own. Therefore, it is important to consider the vertical differentiation of pressure coefficients in coal measure formations, gas content in reservoirs, and natural gas geochemical characteristics.

According to the variation of pressure coefficient of coal measures, gas content and vertical divergence of natural gas geochemical characteristics in Daning-Jixian block, the coal measures from $C_2b$ to $P_2x_8$ can be classified into four independent gas-bearing systems. They are from the top of $C_2b$ to the top of $C_2t_2$, from the bottom of $C_2t_1$ to the top of $P_1s_{2-2}$, from the bottom of $P_1s_{2-1}$ to the top of $P_1s_1$, and from the bottom of $P_2x_8$ to the middle of $P_2x_8$ (Fig. 6). Each of these gas-bearing systems is separated by confining layers, indicating isolation from one another. Additionally, the geochemical characteristics of natural gas differ significantly among these systems, while the pressure coefficients remain relatively consistent within each individual gas-bearing system.

## 4 Sequence stratigraphic analysis of superimposed gas-bearing systems

A complete gas-bearing system comprises three key elements: source rocks, reservoir, and seal rocks (Peters and Cassa, 1994; Ayers, 2002; Law, 2002). The effective source rocks in coal measure mainly include coal and organic-rich mudstone, and the reservoirs mainly include coal seams, coal seams-mudstone interbedding, mud-

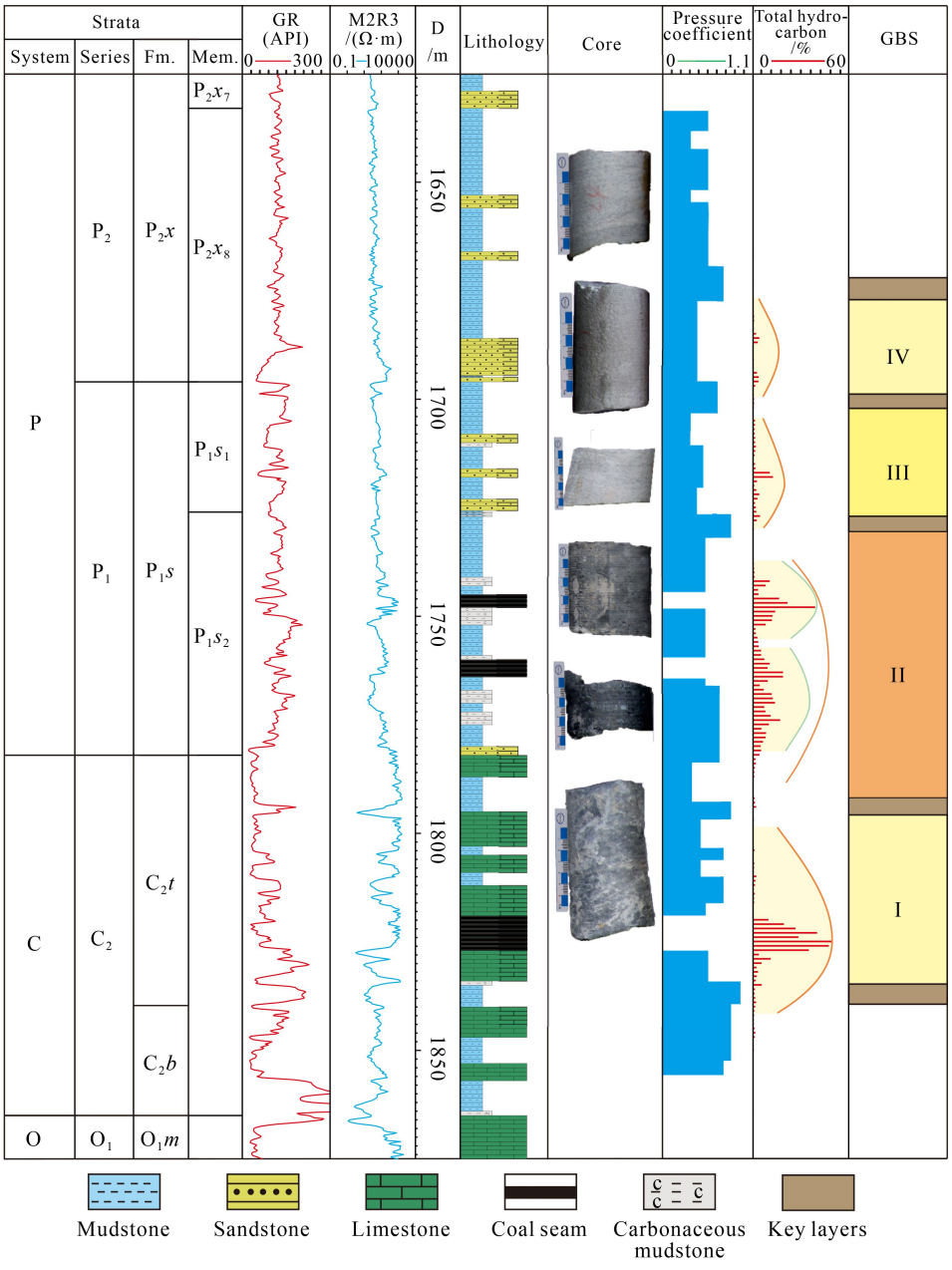


**Fig. 6** Delineation of the gas-bearing system of the coal measures in Daning-Jixian block.

stone-sandstone interbedding, and coal seams-mudstone-sandstone interbedding.

### 4.1 Sequence stratigraphic framework characteristics and sedimentary facies

According to base level recognition standard, the sequence boundaries in the study area are as follow.

1) Regional unconformity surface. The regional unconformities formed by the paleotectonic movement is an isochronous surface, mainly marked by the weathered crustal bauxite on the top surface of the Middle Ordovician limestone.

2) Incised valley (Shanley and McCabe, 1994). Some of the large-scale distributed sandstone bodies in the area are generally undercut valley-fill deposits of low stage, and their base is an erosional unconformity with graded bedding of medium to fine sandstones (Hou et al., 2023a). The study area is dominated by the Jinci Sandstone (K1) at the base of $C_2t$, the Beichakou Sandstone (K7) at the base of $P_1s$, and the Lotopo Sandstone at the base of $P_2x_8$.

3) Maximum flooding surfaces. The coal seams and limestone in $C_2t$ in the study area are important markers.

Because the depositional characteristics of different sedimentary cycles show large differences, which have a great impact on the delineation of the superimposed gas-bearing systems in Daning-Jixian block, it is important to clarify the control of sedimentary cycles on the coal-

measure gas-bearing system. Based on the identification of the base level from $C_2b$ to $P_2x_8$ in Daning-Jixian block and combined with the sequence stratigraphy at the eastern margin of the Ordos Basin (Yang et al., 2005; Yang et al., 2010; Fu et al., 2021), 9 long-term cycles and 14 short-term cycles were delineated (Fig. 7), among which 5 long-term ascending semi-cycles and 4 long-term descending semi-cycles were developed.

The sedimentary environment controls coal accumulation, lithology and diagenetic facies of coal-bearing strata (Lu et al., 2017). Therefore, the identification of sedimentary facies types is the basis for ascertaining the significance of the sedimentary environment on the gas-bearing system of coal measure. By analyzing the data collected from over 50 wells and sedimentary facies markers, two sedimentary facies, four subfacies and seven microfacies were identified from $C_2b$ to $P_2x_8$. The types of sedimentary facies are barrier-coast facies and shallow-water delta facies. The barrier-coast facies mainly develop tidal flats, lagoons and barrier islands. The tidal flat facies can be subdivided into mud flat, sand flat, mixed flat, carbonate tidal flat and peat swamp. The delta front subfacies can be divided into underwater distributary channel, distributary bay, mouth bar and peat swamp (Table 2).

During the SQ2 period, the whole area was dominated by the barrier-lagoon facies, and seawater invaded the study area from the east. Localized carbonate tidal flat facies were developed in the middle of the study area, and barrier sand bars were developed in specific areas (Fig. 8(a)). In the SQ3 period, seawater continued to intrude from the east and south, resulting in the development of barrier-lagoon phase. Two barrier sand bars were developed in the south-east and north-east corners (Fig. 8(b)). During the period of SQ6, seawater retreated. The southern and northern provenance areas

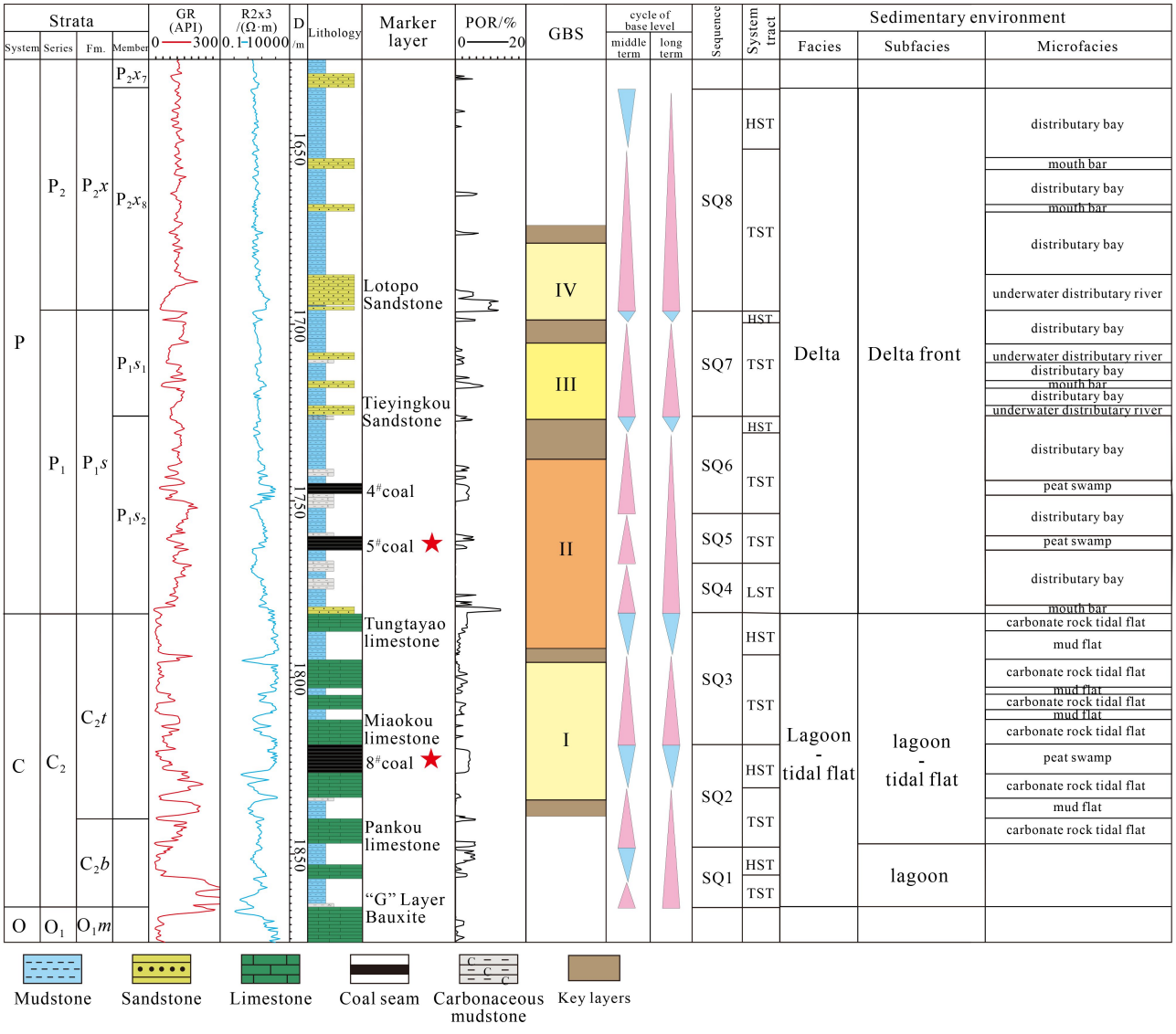


**Fig. 7** Stratigraphic framework and sedimentary phases types in Daning-Jixian block.

**Table 2** Sedimentary facies types from $C_2b$ to $P_2x_8$ in the study area

| Sedimentary system | Sedimentary facies | Sedimentary subfacies | Sedimentary microfacies |
|---|---|---|---|
| Delta | Shallow water delta | Delta front | Underwater distributary channel, distributary bay, mouth bar, peat swamp |
| Barrier coast | Barrier coast | Barrier island | - |
| | | Lagoon | - |
| | | Tidal flat | Mud flat, sand flat, carbonate tidal flat, peat swamp |

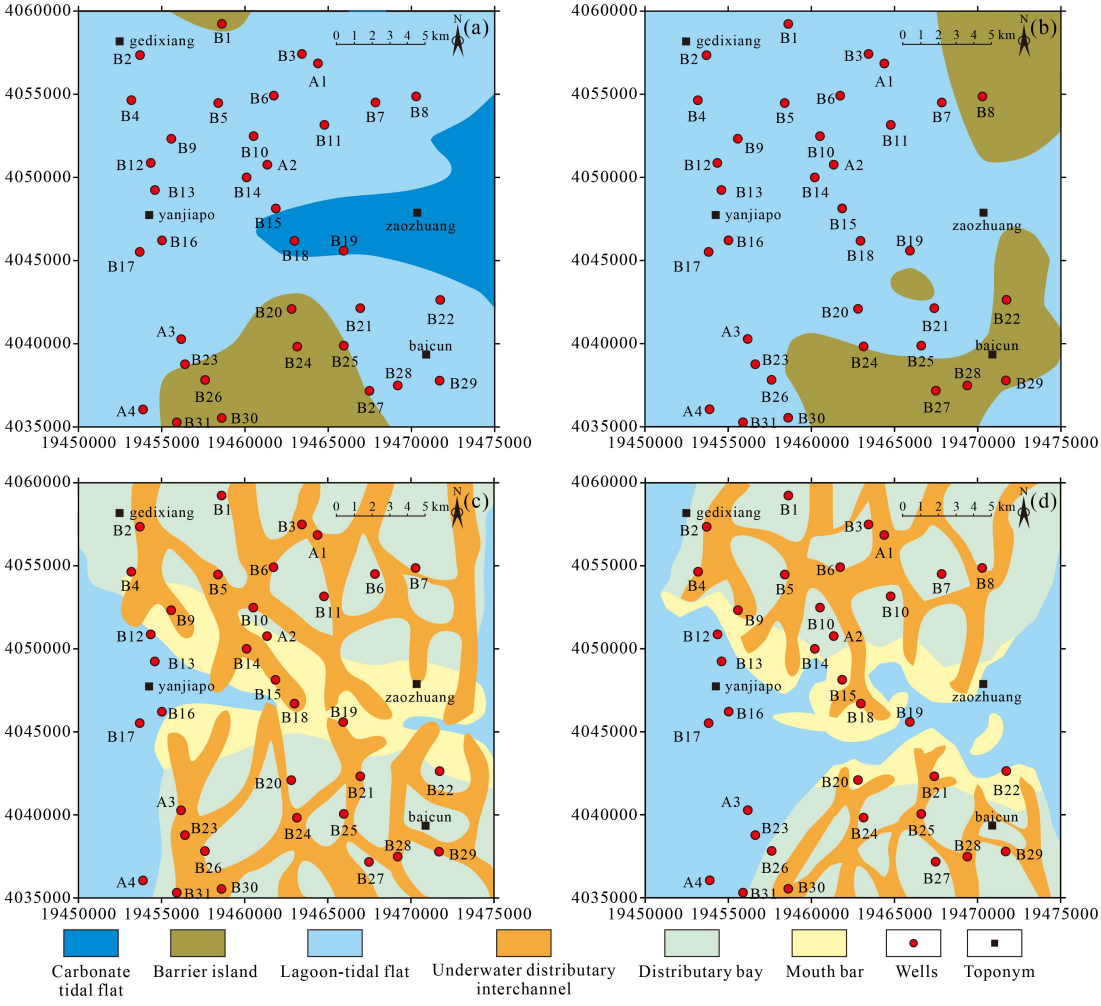


**Fig. 8** Sedimentary microfacies from $C_2b$ to $P_2x_8$ in the study area. (a) SQ2; (b) SQ3; (c) SQ6; (d) SQ8.

were uplifted, and a wide range of delta facies was developed (Fig. 8(c)). In the SQ8 period, the sedimentary environment was similar to that in the SQ6 period, and the delta front facies was developed under the influence of the south-north provenance. The mouth bar is more developed, forming a high-quality sand zone, and the catchment is enriched with far sand bar (Fig. 8(d)).

## 4.2 Sedimentary environment of gas-bearing systems

The coal measures were formed in the sedimentary environment of the terrestrial-marine transitional environment and experienced multiple water transgressive and regressive cycles (Petersen and Andsbjerg, 1996). As a result, the storage capacity of coal and sandstone reservoirs significantly varies, giving rise to distinct assemblages of source, reservoir, and seal rocks. This diversity of rock types ultimately determines the presence of different gas-bearing systems within the area.

According to the assemblage of coal seams, shales, and nearby sandstones, four types of gas-bearing systems are identified.

Type I: System developing multiple coal seams, shales, and sandstone layers. Frequent overlapping of thin source rocks (coal or shale) with adjacent reservoirs increases the contact area, facilitating gas expulsion and conversion

into free gas. In addition, the thin interbedded reservoirs with different lithologies are favorable to the development of natural fractures and the formation of high-permeability superposed reservoirs (Zou et al., 2022). In this case, multiple coal seams and sandstones are superimposed, reflecting the cyclicity of sedimentary environment evolution. The complex changes in the pore structure of coal significantly influence the physical properties of coal reservoirs (Hou et al., 2023b). Coal seams and nearby sandstones act as reservoirs, accumulating hydrocarbon gases generated from coal seams, which are coordinated with the appropriate regional cap rock to accumulate the coal-measure gas (Fig. 9(a)).

Type II: System only developing multiple coal seams and shales. In general, mudstones and siltstones are superior to sandstones, sand-mud interbeds, and carbonates for coalbed methane preservation (Hou et al., 2019). In this case, the sandstone layers are underdeveloped or not developed, which reflects that the sedimentary environment has been in the marsh environment for a long time and the supply of terrigenous detrital is not sufficient. The well-developed coal seams and shales provide ample gas sources, while the thick mudstones offer suitable sealing conditions for coal measure gas preservation (Fig. 9(b)).

Type III: System develops multiple sandstone layers. The scarcity of coal seams and the prevalence of sandstone layers above and below them signify an abundant supply of terrigenous detrital. Hydrocarbon gases from coal are stored directly in nearby sandstones (Fig. 9(c)).

Type IV: System develops multiple limestones or mudstones. The combination is generally formed in the sedimentary environment of carbonate platform with favorable sealing conditions. Limestones are widely developed, while sandstones are less developed. Single coal or shale gas reservoir could form in this type of environment (Fig. 9(d)).

The sediments in the barrier-lagoon facies generally consist of fine clastic rocks and mudstones. The sandstones are mostly found in barrier bars and sand flats,

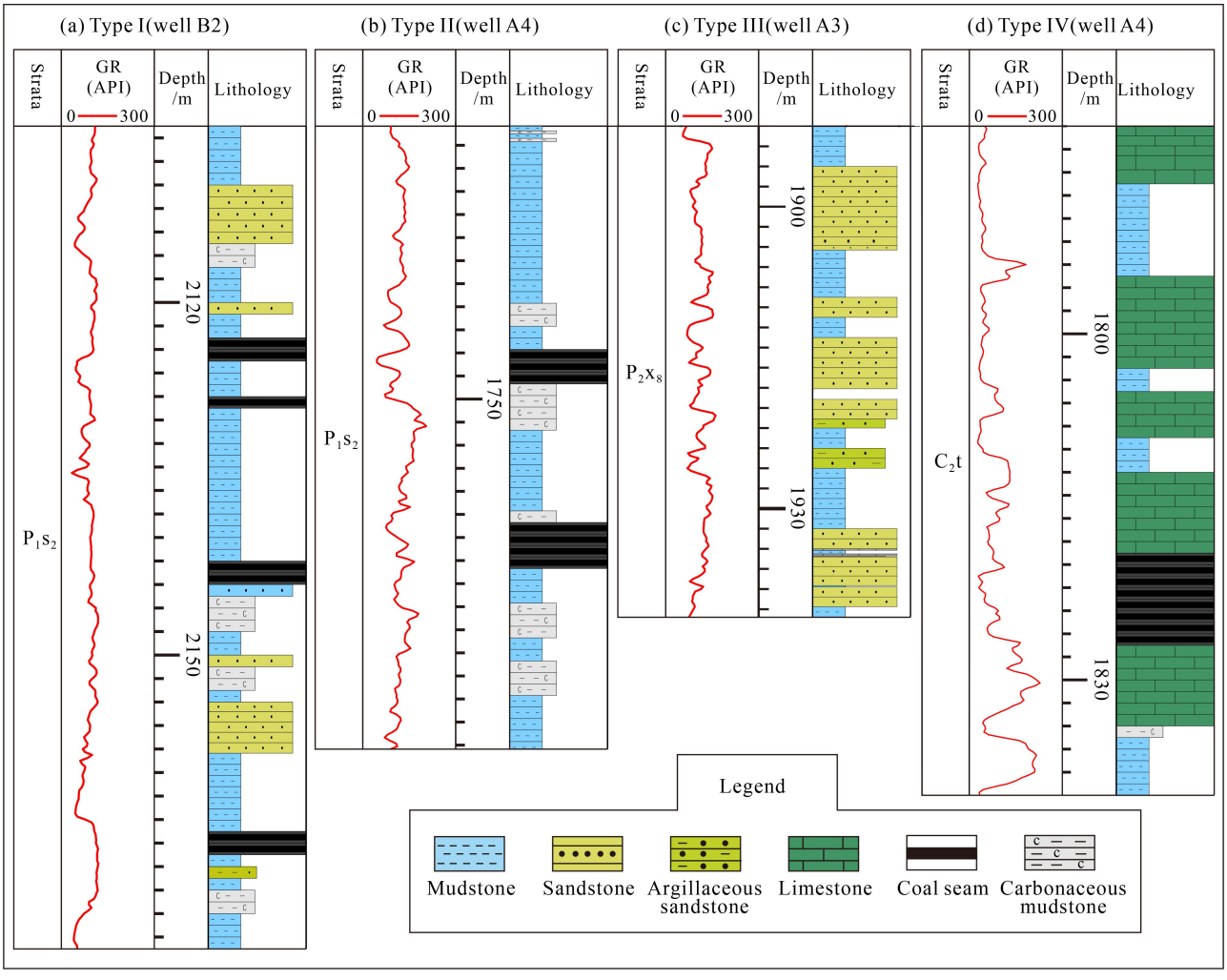


**Fig. 9** Types of gas-bearing systems. (a) type I; (b) type II; (c) type III; (d) type IV.

which are generally located in a few locations. The gas-bearing systems are more likely to form type II assemblages. The mudstone on the roof and floor of coal seams is developed, and the capping ability is strong.

In carbonate tidal flat facies, the coal seam is generally thin and the sandstone is not developed. The gas-bearing systems are more likely to form type IV assemblages. The roof of coal seams is mostly carbonate rock.

In the delta front phases, the underwater distributary bay is a favorable environment for coal accumulation, and the continuity of coal seams is good. At the same time, distributary channel sandbody and mouth bar sandbody are widely developed. The gas-bearing systems are mostly composed of type I and III.

### 4.3 Impact of sequence stratigraphy on distribution of key layers

The degree of superpositionality of gas-bearing systems in coal measures is controlled by the sequence stratigraphic framework (Shen et al., 2016). Through data surveys and the analysis of gas-bearing systems in individual wells within the study area, it has been observed that the strata contain low-permeable mudstone and siderite, known as key layers. These key layers in the gas-bearing systems served as barriers during the formation of independent gas-bearing systems (Shen et al., 2019). The key layers are generally found in close proximity to the maximum flooding surface. This occurrence can be attributed to the weak reducing environment near the maximum flooding surface, characterized by iron-rich, oxygen-poor conditions, limited hydrodynamic activity, and an ample supply of $CO_2$. Such conditions favor the formation of low-permeability mudstone containing siderite. Consequently, it is feasible for key layers to exhibit a continuous distribution within the ascending cycle.

The distribution of the sedimentary system under the restriction of the sequence framework controls the distribution of the independent gas-bearing system. In the lagoon-tidal flat facies, the number of sedimentary cycles is high and the ratio of sand to mud is low. The sediments are dominated by fine-grained clastic rocks, which reflects low depositional environmental energy. Additionally, limestone is more developed and coarse-grained clastic rocks are rare under the influence of seawater. The low permeability mudstone and frequent depositional cycles in this phase impede fluid flow between gas-bearing assemblages and the independent gas-bearing system is well developed. Compared with the lagoon-tidal flat facies area, the delta front facies area has a coarser sediment size and higher sand-mud ratio. The number of sedimentary cycles is low and the thickness of individual cycles is large. the surrounding rock of coal seams acts as a barrier, preventing coalbed methane leakage. These sedimentary characteristics facilitate fluid connections between gas-bearing assemblages and contribute to relatively unified fluid pressure systems.

Five first-order key layers and two locally developed second-order key layers were identified based on the stratigraphic sequence. The first-level key layers are located near the maximum flooding surface of SQ2, SQ3, SQ6, SQ7, and SQ8, respectively, named Ky1, Ky2, Ky3, Ky4, and Ky5 from bottom to top (Fig. 10). Ky1 is located at the bottom of $C_2t$, with a thickness of 2−11 m, and consists of mudstone and silty mudstone. Ky2 occurs at the top of $C_2t$, with a thickness of 2−12 m, and is composed of mudstone, silty mudstone and limestone. Ky3 is located at the top of $P_1s_2$, with a thickness of 3−15 m, and is composed of mudstone and silty mudstone. Ky4 is located at the top of $P_1s_1$, with a thickness of 3−14 m and is composed of mudstone and silty mudstone. Ky5 is located in the central part of $P_2x_8$ and is composed of mudstone and silty mudstone. The secondary key layer is located in the south-west of the study area. The two key layers are located in the period of SQ7 and SQ4, respectively, with a thickness of 2−8 m, and consist of mudstone and silty mudstone. Changes in the pressure coefficient, gas content, and fluid geochemical characteristics of the coal measures are in good accordance with the distribution characteristics of the key layers.

The north-east part of the study area is dominated by delta front sedimentary facies with weak sealing properties and relatively simple gas-bearing systems. In the south-west, the delta front and lagoon-tidal flat overlapped, forming more complex gas-bearing systems (Fig. 10).

## 5 Conclusions

Based on variations of the reservoir pressure coefficient, gas content, and natural gas carbon isotope, the coal measures from $C_2b$ to $P_2x_8$ in Daing-Jixian block can be classified into four independent gas-bearing systems. These systems are identified as 1) from the top of $C_2b$ to the top of $C_2t_2$, 2) from the bottom of $C_2t_1$ to the top of $P_1s_{2\text{-}2}$, 3) from the bottom of $P_1s_{2\text{-}1}$ to the top of $P_1s_1$, and 4) from the bottom of $P_2x_8$ to the middle of $P_2x_8$.

The four gas-bearing systems exhibit different formation combinations and sedimentary environments. Type I system develops multiple coal seams, shales, and sandstone layers. Type II is characterized by multiple coal seams and shales. Type III is dominated by multiple sandstone layers, while type IV is primarily composed of limestones or mudstones. Gas-bearing systems deposited in barrier-lagoon are mainly composed of type II, those deposited in carbonate tidal flats are mostly composed of type IV, and those in the delta front are mostly composed

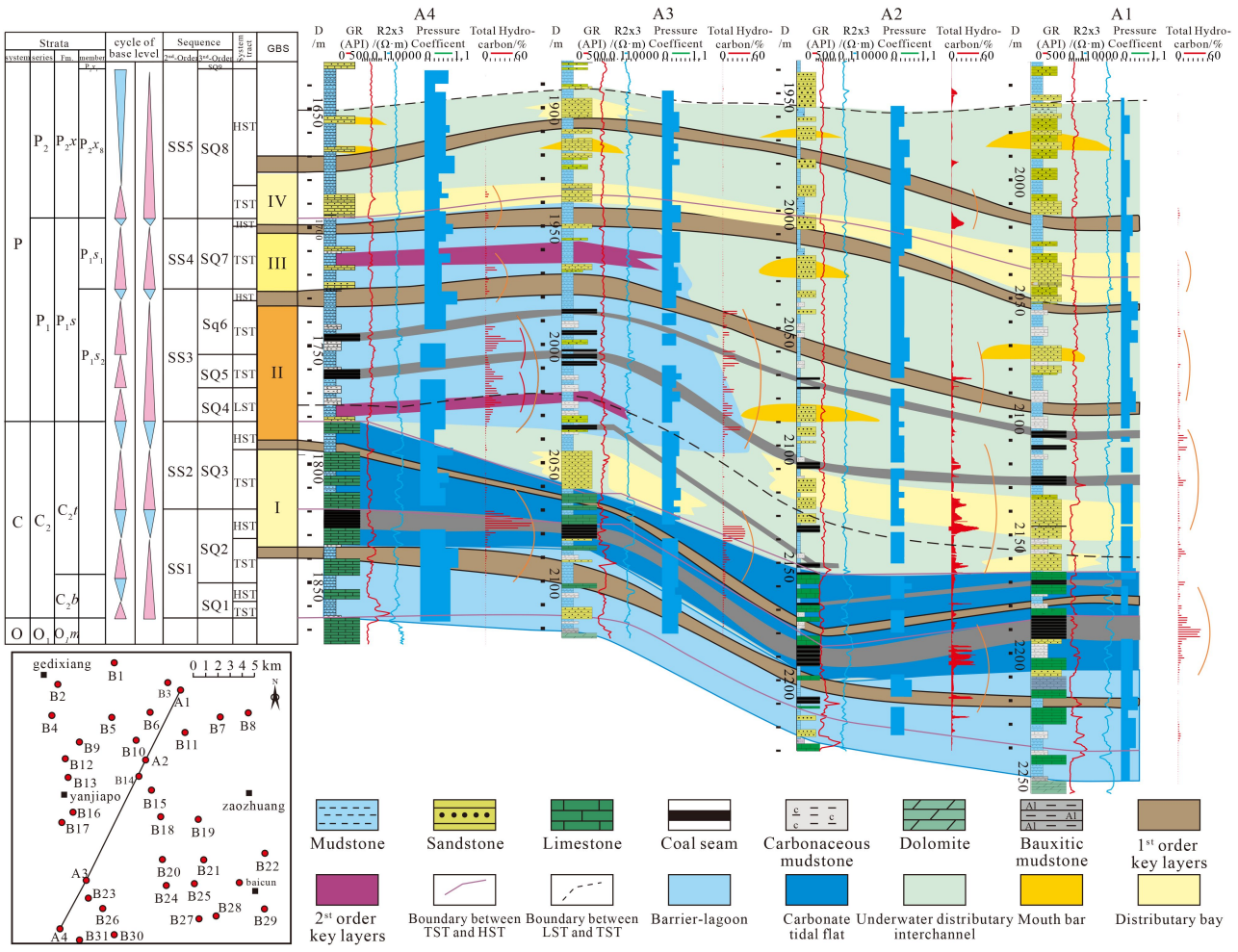


**Fig. 10** Sedimentation control of superimposed gas-bearing systems from $C_2b$ to $P_2x_8$.

of types I and III.

Sequence stratigraphic framework controls the distribution of key layers, which are generally found in close proximity to the maximum flooding surface. The sedimentary environment contributes significantly to the distribution of gas-bearing systems. Compared with the delta interdistributary bay, the tidal flat-lagoon phase has greater water depth and a stronger reducing property. leading to the formation of several key layers. Consequently, the vertical gas-bearing systems located in the overlapped environment of delta front and lagoon in the south-west of the study area are more complex than those located in delta front facies in the north-east of the study area.

**Acknowledgments** This work was supported by the National Natural Science Foundation of China (Grant Nos. 42072198 and 42130802), and the Fundamental Research Funds for the Central Universities (No. 265QZ2021011). The authors would like to thank CNPC for providing important data, experimental test facilities, and the editors and reviewers for their critical comments.

**Competing interests** The authors declare that they have no competing interests.

## References

Allen J P, Fielding C R (2007). Sedimentology and stratigraphic architecture of the Late Permian Betts Creek Beds, Queensland, Australia. Sediment Geol, 202(1): 5–34

Ayers W B (2002). Coalbed gas systems, resources, and production and a review of contrasting cases from the San Juan and Powder River basins. AAPG Bull, 86(11): 1853–1890

Chen S D, Tang D Z, Tao S, Chen Z L, Xu H, Li S (2018a). Coal reservoir heterogeneity in multicoal seams of the Panguan syncline, western Guizhou, China: implication for the development of superposed CBM-bearing systems. Energy Fuels, 32(8): 8241–8253

Chen S D, Tang D Z, Tao S, Xu H, Zhao J L, Fu H J, Ren P F (2018b). In-situ stress, stress-dependent permeability, pore pressure and gas-bearing system in multiple coal seams in the Panguan area, western Guizhou, China. J Nat Gas Sci Eng, 49: 110–122

Cooper J A G, Green A N, Loureiro C (2018). Geological constraints on mesoscale coastal barrier behaviour. Global Planet Change, 168: 15–34

Diessel C, Boyd R, Wadsworth J, Leckie D, Chalmers G (2000). On balanced and unbalanced accommodation/peat accumulation ratios in the Cretaceous coals from Gates Formation, Western Canada,

and their sequence-stratigraphic significance. Int J Coal Geol, 43(1–4): 143–186

Eaton B A (1972). The effect of overburden stress on geopressure prediction from well logs. J Pet Technol, 24(8): 929–934

Flores R M, Sykes R (1996). Depositional controls on coal distribution and quality in the Eocene Brunner Coal Measures, Buller Coalfield, South Island, New Zealand. Int J Coal Geol, 29(4): 291–336

Fu C, Yu X H, Li S L, Peng Z X, Shi S (2021). Carboniferous-Permian transgression/regression mechanisms in the Eastern Ordos Basin and their sea-level spatiotemporal variability: insights from source-to-sink systems. Mar Pet Geol, 123: 104722

Guo C, Qin Y, Wu C F, Lu L L (2020). Hydrogeological control and productivity modes of coalbed methane commingled production in multi-seam areas: a case study of the Bide-Santang Basin, western Guizhou, South China. J Petrol Sci Eng, 189: 107039

Holz M, Kalkreuth W, Banerjee I (2002). Sequence stratigraphy of paralic coal-bearing strata: an overview. Int J Coal Geol, 48(3–4): 147–179

Hou H H, Shao L Y, Tang Y, Li Y N, Liang G D, Xin Y L, Zhang J Q (2023a). Coal seam correlation in terrestrial basins by sequence stratigraphy and its implications for paleoclimate and paleoenvironment evolution. J Earth Sci, 34(2): 556–570

Hou H H, Shao L Y, Tang Y, Li Z, Zhao S, Yao M L, Wang X T, Zhang J Q (2023b). Pore structure characterization of middle- and high-ranked coal reservoirs in northern China. AAPG Bull, 107(2): 213–241

Hou H H, Shao L Y, Wang S, Xiao Z H, Wang X T, Li Z, Mu G Y (2019). Influence of depositional environment on coalbed methane accumulation in the Carboniferous-Permian coal of the Qinshui Basin, northern China. Front Earth Sci, 13(3): 535–550

Jia L, Peng S J, Xu J, Yan F Z (2021). Interlayer interference during coalbed methane coproduction in multilayer superimposed gas-bearing system by 3D monitoring of reservoir pressure: an experimental study. Fuel, 304: 121472

Law B E (2002). Basin-centered gas systems. AAPG Bull, 86(11): 1891–1919

Lei B, Qin Y, Gao D, Fu X H, Wang G G X, Zou M J, Shen J (2012). Vertical diversity of coalbed methane content and its geological controls in the Qingshan Syncline, western Guizhou Province, China. Energy Exploration & Exploitation, 30(1): 43–58

Li Q X, Xu J, Shu L Y, Yan F Z, Pang B, Peng S J (2023a). Exploration of the induced fluid-disturbance effect in CBM co-production in a superimposed pressure system. Energy, 265: 126347

Li S, Qin Y, Tang D Z, Shen J, Wang J J, Chen S D (2023b). A comprehensive review of deep coalbed methane and recent developments in China. Intern J Coal Geol, 279: 104369

Lu J, Shao L Y, Yang M F, Zhou K, Wheeley J R, Wang H, Hilton J (2017). Depositional model for peat swamp and coal facies evolution using sedimentology, coal macerals, geochemistry and sequence stratigraphy. J Earth Sci, 28(6): 1163–1177

Martin A J J, Solomon S T, Hartmann D J (1997). Characterization of petrophysical flow units in carbonate reservoirs. AAPG Bull, 81(5): 734–759

Nowacki D J, Ganju N K (2018). Storm impacts on hydrodynamics and suspended-sediment fluxes in a microtidal back-barrier estuary. Mar Geol, 404: 1–14

Peters K E, Cassa M R (1994). Applied source rock geochemistry. In: Magoon L B, Dow W G, eds. The Petroleum System: From Source to Trap. Tulsa: AAPG Memoir, 93–120

Petersen H I, Andsbjerg J (1996). Organic facies development within Middle Jurassic coal seams, Danish Central Graben, and evidence for relative sea-level control on peat accumulation in a coastal plain environment. Sediment Geol, 106(3–4): 259–277

Powley D E (1990). Pressure and hydrogeology in petroleum basins. Earth Sci Rev, 29(1): 215–226

Raff J L, Shawler J L, Ciarletta D J, Hein E A, Lorenzo-Trueba J, Hein C J (2018). Insights into barrier-island stability derived from transgressive/regressive state changes of Parramore Island, Virginia. Mar Geol, 403: 1–19

Shanley K W, McCabe P J (1994). Perspectives on the sequence stratigraphy of continental strata. AAPG Bull, 78(4): 544–568

Shen Y L, Qin Y, Guo Y H, Yi T S, Yuan X X, Shao Y B (2016). Characteristics and sedimentary control of a coalbed methane-bearing system in Lopingian (Late Permian) coal-bearing strata of western Guizhou province. J Nat Gas Sci Eng, 33: 8–17

Shen Y L, Qin Y, Wang G G X, Guo Y H, Shen J, Gu J Y, Xiao Q, Zhang T, Zhang C L, Tong G C (2017). Sedimentary control on the formation of a multi-superimposed gas system in the development of key layers in the sequence framework. Mar Pet Geol, 88: 268–281

Shen Y L, Qin Y, Wang G G X, Xiao Q, Shen J, Jin J, Zhang T, Zong Y, Liu J B, Zhang Y J, Zheng J (2019). Sealing capacity of siderite-bearing strata: the effect of pore dimension on abundance and micromorphology type of siderite in the Lopingian (Late Permian) coal-bearing strata, western Guizhou Province. J Petrol Sci Eng, 178: 180–192

Su X B, Li F, Su L N, Wang Q (2020). The experimental study on integrated hydraulic fracturing of coal measures gas reservoirs. Fuel, 270: 117527

Su X B, Lin X Y, Zhao M J, Song Y, Liu S B (2005). The upper Paleozoic coalbed methane system in the Qinshui Basin, China. AAPG Bull, 89(1): 81–100

Tang S L, Tang D Z, Tang J C, Tao S, Xu H, Geng Y G (2017). Controlling factors of coalbed methane well productivity of multiple superposed coalbed methane systems: a case study on the Songhe mine field, Guizhou, China. Energy Exploration & Exploitation, 35(6): 665–684

Wang G, Qin Y, Xie Y W, Shen J, Han B B, Huang B, Zhao L (2015). The division and geologic controlling factors of a vertical superimposed coalbed methane system in the northern Gujiao blocks, China. J Nat Gas Sci Eng, 24: 379–389

Wang G, Qin Y, Xie Y W, Wang Z W, Wang B Y, Wang Q, Zhang X Y (2020). Cyclic characteristics of the physical properties of key strata in CBM systems controlled by sequence stratigraphy - An example from the Gujiao Block. Acta Geol Sin, 94(2): 444–455

Wang S, Shao L Y, Wang D D, Sun Q P, Sun B, Lu J (2019). Sequence stratigraphy and coal accumulation of Lower Cretaceous coal-bearing series in Erlian Basin, northeastern China. AAPG Bull, 103(7): 1653–1690

Wang Y, Yang J H, Yuan D X, Liu J, Ma R (2022). Conodont biostratigraphic constraint on the Lower Taiyuan Formation in southern North China and its paleogeographic implications. J Earth Sci, 33(6): 1480–1493

Yang M H, Liu C Y, Lan C L, Liu L, Li X, Zhang K S (2010). Late Carboniferous-Early Permian sequence stratigraphy and depositional evolution in the northeast Ordos Basin, north China. Acta Geol Sin, 84(5): 1220–1228

Yang Y T, Li W, Ma L (2005). Tectonic and stratigraphic controls of hydrocarbon systems in the Ordos Basin: a multicycle cratonic basin in central China. AAPG Bull, 89(2): 255–269

Yang Z B, Qin Y, Wang G X, An H (2015). Investigation on coal seam gas formation of multi-coalbed reservoir in Bide-Santang Basin southwest China. Arab J Geosci, 8(8): 5439–5448

Zhang Y, Li S, Tang D Z, Liu J C, Lin W J, Feng X, Ye J C (2022). Geological and engineering controls on the differential productivity of CBM wells in the Linfen block, southeastern Ordos Basin, China: insights from geochemical analysis. J Petrol Sci Eng, 211: 110159

Zhang Z, Qin Y, Fu X H, Yang Z B, Guo C (2015). Multi-layer superposed coalbed methane system in southern Qinshui Basin, Shanxi Province, China. J Earth Sci, 26(3): 391–398

Zhong G H, Li S, Tang D Z, Tian W G, Lin W J, Feng P (2022). Study on Co-production compatibility evaluation method of multilayer tight gas reservoir. J Nat Gas Sci Eng, 108: 104840

Zou C N, Yang Z, Huang S P, Ma F, Sun Q P, Li F H, Pan S Q, Tian W G (2019). Resource types, formation, distribution and prospects of coal-measure gas. Pet Explor Dev, 46(3): 451–462

Zou Y S, Gao B D, Zhang S C, Ma X F, Sun Z Y, Wang F, Liu C Y (2022). Multi-fracture nonuniform initiation and vertical propagation behavior in thin interbedded tight sandstone: an experimental study. J Petrol Sci Eng, 213: 110417